JOURNAL OF APPLIED ELECTROCHEMISTRY 25 (1995) 34–40

Electrorefining of aluminium scrap from chloride melts

V. SCHWARZ, H. WENDT

Institut für Chemische Technologie der TH Darmstadt, Petersenstrasse 20, D-64287 Darmstadt, Germany

Received 21 February 1994; revised 3 June 1994

The production of aluminium of primary quality from scrap by electrorefining may become an option of strategic importance. Two important requirements are: (i) substantial energy savings compared to electrowinning, and (ii) easy recycling of alloying elements and molten electrolyte without ecological hazards. The use of molten chloride instead of fluoride electrolytes is preferred as emissions are low, purification of contaminated salts in aqueous solution is easy and oxide ceramic materials for cells and diaphragms can be used. The measurement of formal potentials of most important alloying elements shows that only manganese should be expected to cause trouble in electrorefining of aluminium scrap from alkali chloride melts. Preparative batch refining experiments show that all these alloying metals can be easily separated; manganese is very likely because its activity in aluminium is decreased by alloying or compound formation in aluminium. Results with cells divided by alumina diaphragms show that energy consumptions can be kept below 5 kWh $(kg\,Al)^{-1}$.

1. Introduction

The recycling of aluminium scrap today is performed by remelting and mixing with primary aluminium and amounts to 30% of the total consumption. The percentage of recycled scrap is increasing slowly but steadily. Electrolytic scrap refining producing aluminium of primary quality would enable the aluminium industry in the future to increase the amount of recycled scrap in the total consumption of aluminium to any desired degree within the range 30–100%. Electrorefining of aluminium with solid metal in low temperature melts seems not to be technically feasible, although it had been demonstrated by Pemsler and Dempson [1], to work on laboratory scale. It is, however, severely hampered by the formation of dendritic deposits.

Electrorefining of aluminium producing metal of 99.99% quality and better is performed today with liquid aluminium cathodes and anodes according to Hoope's three-layer process [2], which works with a fluoride electrolyte but with energy consumptions in the range 10–15 $kWh\,kg^{-1}$, which almost matches that of primary aluminium production. Sullivan and coworkers [3] have shown that highly contaminated aluminium alloys containing only 70% Al can be electrolytically refined to an extent that enhances the contaminant concentration by a factor of three in the anode; even so, they obtained purities of the refined aluminium of 99.6%, matching that of primary aluminium quality. They used mixed fluoride/chloride melts and a chloride melt in a divided cell with a diaphragm and a three layer cell according to Hoope's principles. However, in both cells the energy consumption was too high.

2. Aims of and means for electrolytic refining of aluminium scrap

Low energy consumption, for example below 5 $kWh\,kg^{-1}$ (corresponding to a cell voltage of 1.3 V and less) for aluminium scrap refining at current densities of more than 0.1 $A\,cm^{-2}$, would be a necessity for commercially viable scrap electrorefining. This can only be achieved if the cell design would allow for electrode distances of no more than a few millimetres and cell resistances of less than 2 or preferably as low as 0.5 $\Omega\,cm^2$.

Conductivities of the usual melts (alkali fluorides and chlorides) at 700° C (i.e. 40° above the melting point of aluminium) are between 2 and 6 $\Omega^{-1}\,cm^{-1}$ [4]. Such low cell resistances may therefore only be obtained if an electrolyte-flooded diaphragm of millimetre thickness separates the two electrodes of molten metal. The morphology of the sintered porous oxide ceramic diaphragm must prevent short circuiting of the electrodes by preventing the molten metal from penetrating the diaphragm. This diaphragm also has to allow easy exchange of the electrolyte which fills the interelectrode gap, for instance by gravity flow, as depicted schematically in Fig. 1(a). Fray's proposal [5] of the so-called recessed channel cell, using as diaphragm a fabric of oxide ceramic fibres or a porous sintered material, offers a second possibility of narrow interelectrode gap cell with easy exchange of electrolyte and molten metal. For such divided-cell design, in which both liquid electrode metals touch the diaphragm, electronically conducting diaphragms are excluded. Alumina is the diaphragm material which is intrinsically most consistent with the aim of preventing any contamination of the

0021-891X

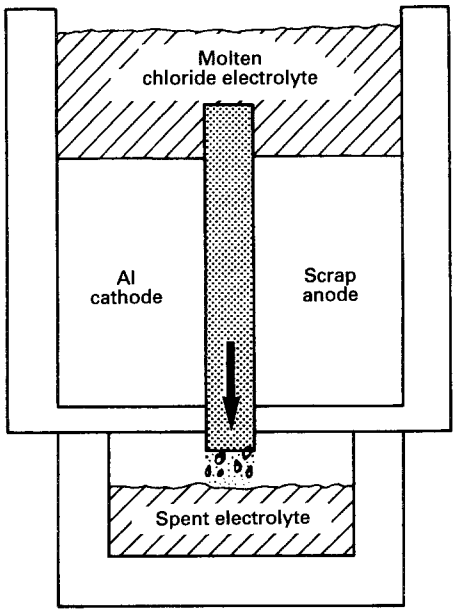

Fig. 1. Schematic of divided refining cell in which the electrolyte contents of the diaphragm is continuously exchanged by gravity-driven flow.

refined metal by construction materials. The solubility of Al_2O_3 in chloride melts, in contrast to fluoride melts, is almost nil. Chloride melts are also easier to purify and to recycle than fluoride melts by dissolving them in water and recovering the material by purification in, and recrystallization from, aqueous solutions.

It is the aim of this paper to report on (i) the determination of the voltage series of the alloying metals of aluminium in chloride melts and (ii) to investigate electrolytic refining of model alloys from chloride melts in divided laboratory scale cells equipped with sintered porous alumina diaphragms. The aim is also to establish a basis for further R & D work by supplying data on the energy consumption of Al-refining in such cells.

3. Experimental details

All experiments reported in this paper refer to a temperature of 700° C although refining experiments were also performed at temperatures below the melting point of aluminium (660° C). They showed, that electrodissolving and depositing solid aluminium is not a reasonable option for scrap refining as the metal always deposits in dendritic and pyrophorous form, and can be remelted only with difficulty.

Three different types of experiments had been performed:

(i) Cyclic voltammetry of deposition/dissolution of alloying elements from chloride melts at different electrode materials.

(ii) Measurements of equilibrium potentials of these metals.

(iii) Electrolytic refining of alloys in divided cells from chloride melts in closed steel vessels containing an Al_2O_3-crucible with the chloride melt, and protected in a quartz cylinder situated within the steel vessel.

All chemicals used were of PA (Merck) grade. The investigations were performed in a tubular quartz furnace equipped with a semitransparent gold-covered outer heat shield made of a quartz tube in which a stainless steel tube was inserted containing the electrolyte cell. The stainless steel tube whose upper part was water cooled was closed by a graphite lid. Al_2O_3-crucibles, forming the electrolysis cells proper, were cylindrical, of 4 cm diameter, 15 cm height with a wall thickness of 2 mm.

An aluminium reference electrode was constructed from a small alumina-vessel equipped with a Luggin capillary, also of Al_2O_3, which contained a pool of liquid aluminium and molten mixtures of LiCl and NaCl containing 10^{-3} M $AlCl_3$. A tungsten wire served for connecting the Al-pool to the lead which was connected to the voltmeter or potentiostat. As the diameter of the Luggin capillary was much wider than the usual capillary tips, namely 2 mm, in contrast to a tenth of a millimetre, which is usual with Luggin capillaries made of glass, its tip could not be fixed at a distance of closer than 2 mm in front of the electrode. Therefore the *IR* potential drop could not be neglected.

Current voltage curves in the cyclic voltammetric measurements were corrected by the interruption technique. Metal electrodes made of rods of Mg, Mn, Si, Fe and Cu and a pool of liquid zinc, which was used to measure equilibrium potentials, were all at least 99% pure. Graphite rods, at which cyclic voltammetric measurements were performed, were of PT-2114 quality, supplied by Deutsche Carbone. The graphite contained less than 20 p.p.m. ash, with iron and calcium being the most prominent contaminants in concentrations of less than 5 p.p.m. each.

Two different types of alumina diaphragm were used:

(i) quality P80 of Königliche Porzellan Manufaktur, Berlin, Al_2O_3 content 85%, porosity 50% and average pore radius: 30 μm, thickness: 3 to 5 mm;

(ii) quality AL25, of Fa. Friedrichsfeld, Mannheim, Al_2O_3 content: 99.7%, porosity 25%, pore radius: between 10 and 20 μm, thickness 5 mm.

The highly porous diaphragm of type (i) was unstable. It contained SiO_2 as a sinter aid which was reduced in longer experiments, whereupon the material disintegrated by formation of silicon. Therefore the final electrorefining experiments were performed exclusively with diaphragms of type (ii).

The diaphragms, which fitted almost tightly to the vertical cross section of the alumina crucibles were glued to their interior with alumina paste.

The $AlCl_3$ of PA grade (Merck) contained more than 6000 p.p.m. $FeCl_3$ which could not be removed by resublimation. Therefore $AlCl_3$ always introduced sizeable amounts of iron into the electrorefining experiment.

Trace impurities in the purified metal were

Table 1. Composition of model alloys in wt %

	Cast alloy scrap	*Wrought alloy scrap (AlMg4.5)*
Al	89	94.2
Mg	0.9 ± 0.2	4.73
Si	4.7 ± 0.1	0.06
Cu	4.1 ± 0.1	–
Mn	0.4 ± 0.1	0.78
Fe	0.3 ± 0.1	0.18
Zn	0.6 ± 0.1	0.01
Ti	–	0.01

determined by spark spectroscopy in the analytical laboratory of Vereinigte Aluminiumwerke, Bonn.

4. Results

4.1. *Definition of model alloys*

There is a distinction between aluminium wrought alloys and cast alloys. Wrought alloys contain not much more than 5% alloying elements: mainly magnesium (4 to 6 wt %), manganese (0.5 to 1 wt %) and some iron (0.1 to 0.3 wt %). Cast alloys contain more than 10 wt % alloying elements, the most abundant being silicon and copper (both up to 5%) followed by magnesium (1 wt %), Zn (~ 0.5 wt %), manganese and iron (both less than 0.5 wt %). Table 1 shows a typical composition of a cast and a wrought aluminium alloy (the first being a 1 : 1 mixture of GB-AlSi9Cu3 and AlMg2.3, the wrought alloy being standard alloy AlMg4.5) which had been used in this investigation for electrorefining experiments.

4.2. *Definition of the electrolyte*

According to Table 2 the conductivities of alkali chlorides and fluorides increase from potassium to lithium and are higher for fluorides than for chlorides. Therefore LiCl containing $AlCl_3$ or NaF containing AlF_3 is preferred as the electrolyte for electrorefining. However, fluorides have to be excluded as there is no insulating oxide ceramic material known which can serve as a container, and diaphragm material in particular, which would be insoluble in this melt. LiCl has to be excluded, as the vapour pressure of $AlCl_3$ dissolved in this electrolyte is known to be high, ranging from 0.15 to 0.24 bar above LiCl melts at 700° C containing from 5 to 20 mol % of $AlCl_3$ [6].

The ALCOA-electrolyte is a good compromise

Table 2. Specific conductivities, $\kappa/\Omega^{-1}\,cm^{-1}$, of alkali fluoride and chloride melts at 700 °C [4]

	Chloride	*Fluoride*
Li	6.2	5.8*
Na	3.3*	4.1*
K	1.9*	3.3*

* Extrapolated below the respective melting point to 700° C.

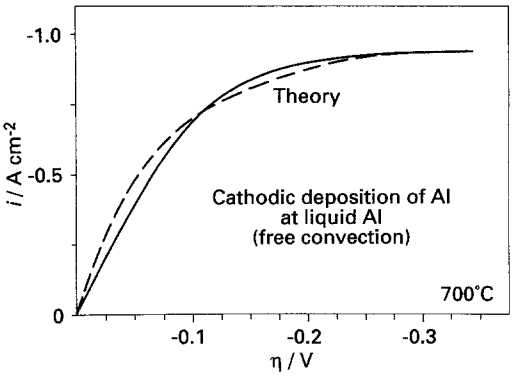

Fig. 2. Current/voltage curve of aluminium deposition from a NaCl/LiCl/$AlCl_3$ melt (ALCOA–electrolyte) under the condition of natural, thermal convection.

containing a mixture of LiCl/NaCl in a molar ratio of 4 : 5 and $AlCl_3$ in variable concentrations ranging from 5 to 15 mol %. At 700° C this mixed electrolyte exhibits $AlCl_3$ pressures from 37 to 55 torr only and relatively high conductivities of 3.53 (5 mol %) and $2.81\,\Omega^{-1}\,cm^{-1}$ (15 mol %) [6]. For refining experiments 15 mol % $AlCl_3$ were used in the electrolyte in order to avoid mass transport limitations at the cathode. Melts containing 15 mol % of $AlCl_3$ correspond to a volume related concentration of approximately 3.9 M $AlCl_3$.

4.3. *Voltammetric investigations*

4.3.1. Current voltage curves of aluminium dissolution and deposition. Figure 2 depicts the *IR*-corrected current voltage curve of cathodic aluminium deposition on an aluminium pool under the condition of free thermal convection measured in a melt containing 10 mol % of $AlCl_3$. Cathodic mass transport limited current density occurs and the broken line compares the theoretical curve according to Equation 1 with the actually measured one

$$i = i_l\{1 - \exp(-v_e F/RT)\} \qquad (1)$$

The deviations between observed and predicted potentials are less than 15 mV and may be due to incomplete *IR*-compensation. The cathodic curve and the respective curve for anodic aluminium dissolution confirm reports in the literature that cathodic Al-deposition and dissolution in chloride melts is a fast, kinetically unhindered process [7, 8].

4.3.2. Cyclic voltammetry of cathodic deposition/anodic dissolution of alloying metals. Three different electrode substrates (Au, C and W) were used for cyclic voltammetric investigations. The aim was to find for each metal a substrate which did not influence the respective voltammogram by compound formation. In each case the electrolyte did not contain aluminium chloride, but only LiCl/NaCl, in order to avoid codeposition of aluminium in the case of formation of aluminium alloys with sizeable negative Gibbs enthalpies (compare for instance cathodic Mn/Al codeposition [9]).

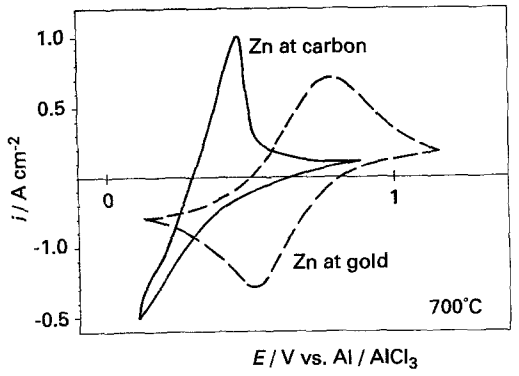

Fig. 3. Voltammogram of zinc deposition/dissolution on gold and graphite electrodes. Due to alloy formation on gold electrodes, the current voltage curve is shifted to more positive potentials.

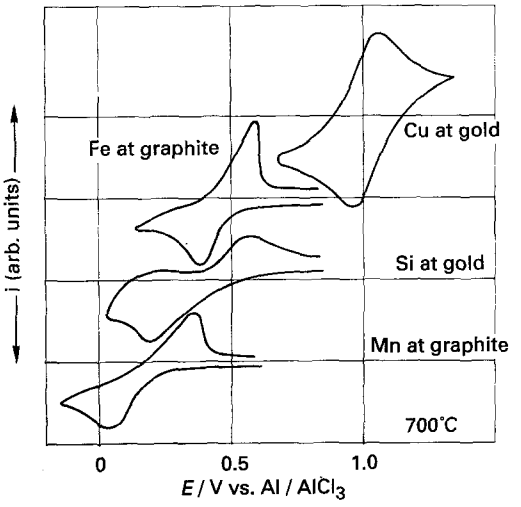

Fig. 4. Voltammograms of Cu, Si, Fe and Mn at different cathode materials.

An example of compound formation of the deposited metal and the electrode substrate is shown in Fig. 3, where the continuous cyclic voltamograms of zinc at gold and graphite electrodes are compared. Zinc is deposited on gold at a potential which differs from the deposition potential on graphite by approximately +0.3 V, due to the relatively fast formation of the intermetallic compound Au_3Zn whose Gibbs free energy may be estimated from the potential difference to be $-57.9\,kJ\,mol^{-1}$ at 700° C.

It should be mentioned, however, that the value found in the literature for the formation enthalpy is almost twice as high, namely $-90\,kJ\,mol^{-1}$ [10]. The deposition of aluminium on gold also occurs with an anodic potential shift of $+0.45 \pm 0.02$ V, very likely due to the formation of the intermetallic compound $AuAl_2$ which has a Gibbs free energy of $260 \pm 15\,kJ\,mol^{-1}$ (according to the binary phase diagram $AuAl_2$ is by far the most stable intermetallic compound [11] in the Au/Al-system).

Figure 4 shows the cyclic voltammograms of Mn, Fe, Si and Cu, the latter being the most noble alloying metal. The voltammograms were measured at tungsten, carbon or gold electrodes, the chosen substrate not forming any intermetallic compound with the respective metal. Copper is completely miscible with gold but the excess heat of mixing is negligible. The melts contained the respective metal chlorides in concentrations ranging from 5×10^{-5} to $1 \times 10^{-4}\,mol\,cm^{-3}$.

Most of the metals are dissolved in the two valent state, iron in three valent and silicon in four valent state. Silicon is added in the form of the complex fluoride K_2SiF_6. This salt dissolves, the SiF_6^{2-} complex transforms by ion-exchange to $SiCl_6^{2-}$ and this decomposes by release of silicon tetrachloride. Therefore solutions of K_2SiF_6 are not stable in chloride melts but their Si-content steadily decreases. As equilibrium potential of the respective metal (as a reasonable approximation) the arithmetic means of the anodic and cathodic peak potentials of the respective voltammograms were chosen which, with the exception of copper at gold, typically have an irreversible character.

Table 3 collects these equilibrium potentials together with the respective concentrations of the salt. Also, the predicted concentration dependence, $dE/d\log c$, of the respective metals are given. Silicon is an exception because its concentration due to the volatility of $SiCl_4$ is not well defined. For four-valent silicon, however, the equilibrium potential is least dependent on concentration, as it changes with concentration by less than 50 mV per decade at 700° C, so that the inaccuracy in determining the formal potential is comparable to that of the two-valent metals.

Table 3. Equilibrium and formal potentials (convention: $c(MeCl_n) = 1 \times 10^{-3}\,mol\,cm^{-3}$) of different metal/metal chloride couples measured in LiCl/NaCl (35/45 mol/mol) melts at 700 °C (Reference Al/AlCl$_3$, $10^{-3}\,mol\,cm^{-3}$)

Metal/metal chloride	*Equi./pot. E/mV* *	*At. conc. c/mol cm^{-3}*	*Electrode material*	*E formal pot. E/mV*	*dE/log c /mV (dec)$^{-1}$*
$Mg/MgCl_2$	-950 ± 30	1.03×10^{-4}	W	-880 ± 20	97
$Mn/MnCl_2$	$+180 \pm 20$	4.06×10^{-5}	Au	$+220 \pm 20$	97
$Zn/ZnCl_2$	$+350 \pm 30$	2.44×10^{-5}	C	$+400 \pm 20$	97
Si/K_2SiF_6†	$+450 \pm 50$	10^{-5} to 10^{-4}†	Au	$+450 \pm 20$	48
$Fe/FeCl_3$	$+450 \pm 50$	2.86×10^{-5}	Au	$+540 \pm 20$	65
$Cu/CuCl_2$	$+850 \pm 30$	1.11×10^{-5}	C	1090 ± 20	97

* All potentials vs $AlCl_3$ $10^{-3}\,mol\,cm^{-3}$ in LiCl/NaCl melt.
† K_2SiF_6 decomposes in the chloride melt forming mixed SiFCl-complexes followed by release of $SiCl_4$.

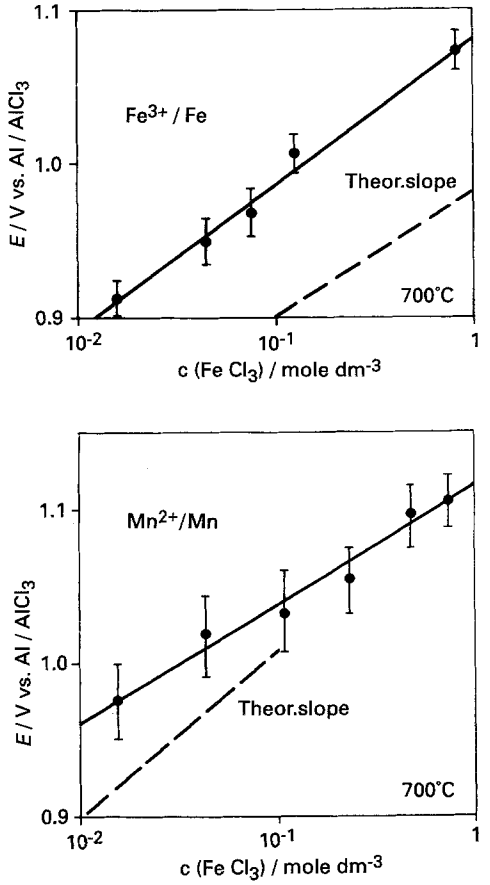

Fig. 5. Concentration dependence of the equilibrium potential of (a) the $MnCl_2/Mn$ and (b) of the $FeCl_3/Fe$ electrode in NaCl/LiCl melts.

4.4. *Measurement of the equilibrium potentials of the alloying elements*

Rod electrodes of 99.9% purity of the alloying elements Mg, Mn, Zn, Fe and Cu were used to measure their equilibrium potentials in NaCl/LiCl melts containing the respective metal chlorides in six different concentrations ranging from 2×10^{-5} to 5×10^{-4} mol cm^{-3}. Repeated readings are reproducible within ± 30 mV.

Figure 5(a) and (b) show the results for manganese and iron. These experiments allow the formal potentials of the respective metal/metal chloride couple to be obtained. The formal potential (different from the normal convention in melts, which refers to the pure metal salt, i.e. mole fraction $x = 1$) refers in the present case to a volumetric concentration of the dissolved salt of 10^{-3} mol cm^{-3} or 1 M. Figure 5(a) and (b) depict the least square linear log concentration/potential correlation and compares it with the theoretical slope $2.3\,RT/v_eF$ (v_e is 2 for $MnCl_2$ and 3 for $FeCl_3$). Table 3 shows the formal potentials measured against an aluminium electrode in LiCl/NaCl melts containing 10^{-3} mol cm^{-3} of $AlCl_3$, and the theoretical slopes $dE/d\log c$ which allows calculation of the equilibrium potential of the respective pure electrode metal at any desired metal chloride concentration in LiCl/NaCl melts at 700° C.

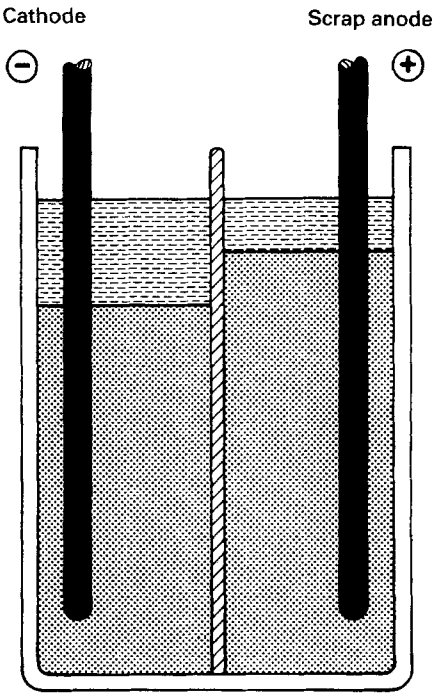

Fig. 6. Schematic of the electrorefining cell divided by an alumina diaphragm used in the present work.

5. Electrorefining experiments

The electrorefining experiments had two different aims: (i) to find a cell design, with sufficiently low cell resistance and (ii) to investigate the effective purification effect achieved in long term refining processes in which nine tenths of the metal is anodically dissolved and cathodically recovered.

5.1. *Different cell designs*

Three different cell designs were compared:
(a) Divided cell with Al_2O_3 diaphragm of 5 mm thickness soaked with the electrolyte (Fig. 6).
(b) Three-partitioned cell containing a bipolar aluminium electrode between the anode and the cathode, all three electrodes separated from each other by electrolyte flooded alumina diaphragms.
(c) Cell with EDE-(electrode/diaphragm/electrode) geometry established by backing a brittle electrolyte-flooded diaphragm of 2 mm thickness from both sides by porous, aluminium flooded carbon plates.

According to the measured current voltage curves the different cells had the surface specific resistances: 1.8, 3.6 and 3.6 Ω cm^2. Obviously the simple, divided cell, as expected, is at an advantage and was used for most of the further experiments with the exception of trying cell type b for obtaining improved purity of the refined aluminium.

The anode initially contained up to 80 g alloy and was oxidized consuming sufficient current to dissolve 90% of the initially present nonnoble metals aluminium and magnesium. The amount of anode metal dissolved, and cathode metal deposited, was determined gravimetrically and the contents of the

Table 4. Comparison of anode and cathode composition (wt %)

	Anode (initially)	*Cathode 1*	*Cathode 2*	*Cathode 3*	*Average*	
	$c_{i,0}$	c_i	c_i	c_i	c_i	c/c_0
Si	4.7	0.00361	0.0315	0.0374	0.055	1/140
Fe	0.3	0.0908	0.1032	0.0800	0.091	1/3.3
Cu	4.1	0.0002	0.0013	0.0017	0.001	1/4100
Mn	0.4	0.0061	0.0198	0.0098	0.012	1/33
Mg	0.9	0.0008	0.0010	0.0010	0.0010	1/900
Cr	0.01	0.0007	0.0006	0.0007	0.0007	1/14
Zn	0.6	0.0061	0.0198	0.0089	0.012	1/50
Al	88.99	99.89	99.82	99.86	99.86	

different metals in the anode and cathode were analysed after termination of the experiment. Applied current densities ranged from 0.3 to 0.5 A cm^{-2}. At 0.5 A cm^{-2} the cell voltage was 0.9 ± 0.15 V.

Table 4 shows the results of three typical experiments which allow the precision and reproducibility of such laboratory scale refining experiments to be evaluated. The refining yields a purified metal of 99.86% from 89% aluminium cast alloy, a quality better than primary aluminium, which does not exceed 99.7% purity. The results obtained with wrought alloys were even better.

Table 5 shows the results of two experiments in which aluminium of primary alloy quality was electrorefined with the aim of producing ultrapure aluminium.

Both Tables 4 and 5 show the concentration of alloying elements initially present in the anode metal and eventually found in the cathode, the latter being corrected for the dilution caused by the initial presence of 10 g of 99.99% aluminium.

6. Discussion

Analysis of the data of Table 4 reveals that the purification or depletion factor, c_i/c_0, for iron is particularly poor. Iron, next to copper, is the noblest metal and should have a depletion factor comparable at least to that of silicon. The reason is obvious: iron is contained in the electrolyte as the aluminium chloride used contains more than 6000 p.p.m. iron.

It is unexpected that manganese, having a formal potential closest to that of the aluminium electrode, has a remarkably high depletion factor of 1/33. This is certainly caused by strong reduction of the activity of this metal in aluminium, as the binary phase diagram of Mn/Al reveals that several aluminium rich compounds are formed, such as $MnAl_6$ and $MnAl_4$. Recent reports on the codeposition of aluminium and manganese from chloride melts confirm this finding [9]. Magnesium as the least noble metal, as expected, is reliably separated by the electrorefining process and accumulates in the electrolyte; the anode contains almost no magnesium after the experiment.

Assuming that the depletion factor of iron is at least as low as that of silicon, a cathode quality of 99.97% would be obtained, a value indicating that it could be possible to obtain 99.99% or even higher grade aluminium by primary aluminium refining in chloride melts. Experiments (see Table 5) with the aim of obtaining high purity aluminium from primary aluminium, however, showed that the depletion factor for all metals increases, i.e. deteriorates at low concentrations, yielding only 99.94% aluminium. An exception seems to be iron, as its depletion factor is lower, i.e. better, than that obtained with electrorefining of the wrought alloy. In this case an electrolyte was used which was purified by pre-electrolysis. Therefore, further efforts would have to be expended to achieve this target. The highest cell voltages observed with current densities of 0.5 A cm^{-2} were below 1.3 V. Therefore the energy demands for scrap electrorefining at this current density was lower than 5 kWh per kg of aluminium.

Table 5. Comparison of anode and cathode composition (wt %) for electrorefining of primary aluminium

	Anode (initially)	*Cathode 1*	*Cathode 2*	*Average*	
	$c_{i,0}$	c_i	c_i	c_i	c/c_0
Si	0.056	0.0064	0.0362	0.0213	1/2.6
Fe	0.18	0.0392	0.0209	0.03	1/6
Cu	0.004	0.0006	0.0002	0.0004	1/10
Mn	0.003	0.0022	0.0011	0.0017	1/1.76
Mg	0.002	0.0002	0.0013	0.0008	1/2.5
Zn	0.004	0.0011	0.0012	0.0012	1/3.3
Al	99.75	99.945	99.959	99.952	

Acknowledgements

The authors are indebted to the Commission of the European Communities for financial support under the programme 'Recycling of nonferrous metals', contract MAIR-0015C and to Vereinigte Aluminiumwerke, in particular to Drs Lossmann and Wilkening, for their considerable help in performing the chemical analysis of the refined metal.

References

[1] J. P. Pemsler and M. Dempsey, 'Electrorefining of Aluminium', Gouv. Rep. Announce, NSF/CPE-81012, B.P. 81-243693 (1981).

[2] W. Hirt, H. K. Johnson, S. Wilkening and S. Winkhaus, 'Aluminium und Magnesium', *in* H. Harnisch, R. Steiner and K. Winnacker Hergb., 'Chemishe Technologie', vol. 4, Carl Hanser Verlag, München, Wien (1986) pp. 235ff.

[3] T. A. Sullivan and R. L. De Beauchamp, 'Recovery of aluminium, base and precious metal from electronic scrap', Bureaux des Mines, RI-7617, BP-2090 (1971).

[4] A. Klemm, 'Ionic mobilities' *in* 'Advances of Molten Salt Chemistry', vol. 6 (edited by G. Mamantov, C. B. Mamantov and J. Braunstein), Elsevier, Amsterdam (1987).

[5] D. J. Fray, *British Patent Application* 130 821 (1986).

[6] H. Linga, H. Øye and K. Motzfeld, *Ber. Bunsenges. Phys. Chem.* **85** (1981) 1132.

[7] R. Tunold and R. Ødegard, 'Kinetics of the deposition of aluminium from chloride melts', *in* Proceedings Vth International Symposium on Molten Salts (edited by M. L. Saboungi, K. Johnson, D. S. Newman and D. Inman), *Electrochem. Soc. Proc.* vol., Proceedings Volume 86–1 (1986) pp. 408*ff*.

[8] R. Ødegard, A. Bjørgum, A. Sterten, J. Thonstad and R. Tunold, *Electrochim. Acta* **27** (1982) 1595.

[9] T. Takayama, H. Seto, J. Uchida and S. Hinotani, *J. Appl. Electrochem.* **24** (1994) 131.

[10] W. Biltz, G. Rohloffs and H. U. v. Vogel, *Z. anorg. allgem. Chemie* **220** (1934) 113.

[11] Aluminium–Gold, *in* 'Constitution of Binary Alloys' (edited by M. Hansen and K. Anderko), McGraw-Hill, New York (1958) pp. 68*ff*.